ON POSSIBILITIES OF TV BEAM DIAGNOSTICS TECHNIQUE, USING OPTICAL RADIATION FROM FLYING WIRE SCANNER

V.P.Novikov, E.V.Serga, A.V.Kharlamov
Institute for High Energy Physics, 142284, Protvino, Moscow Region, USSR

Abstract: A new technique for beam diagnostics using optical radiation, arising from a charged particle interaction with the wire crossing the beam, is proposed. Possibilities of using optical transition are considered.

Introduction

The scanning technique, using secondary particles arising from the thin wire scanning the beam, has widely been exploited at CERN, FNAL [1,2] for beam diagnostics. The measurements of secondary particles allow one to obtain the beam profile. The thin wire does not practically worsen the beam parameters (intensity, momentum, emittance). One of the disadvantages of the given technique is the radiation heating and deterioration of the wire in the high intensity beams. To decrease the heating the authors of work [3] used a wire with a small diameter 5 μm. An increase of the velocity with which the scans the beam is another way to decrease the heating. For instance, the velocity achieved at the CERN PS [4] is 20 m/s. However the error in determining the beam position considerably increases with the growth of the velocity. The scanning of the beam with the wire is also accompanied by the optical transition radiation (OTR), luminescence, Cherenkov radiation. In this case the total number of the photons emitted is greatly larger than the number of secondary particles. Under large heating there aslo appears heat emission.

The present work is devoted to the description of the optical radiation detection with the help of TV camers. The possibilities of using the luminescent radiation and OTR for the beam detection are studied here. The threshold sensitivity for the beam diagnostics are being determined for the IHEP, CERN, FNAL and KhPTI machines.

Measurement Technique

The optical radiation, projected onto the target of the vidicon (Fig.1a). The TV camera has a controlled storage time on the vidicon with cadmium selenide target, and it starts operating in the accumulation mode at the instant of time when the wire enters the fiducial area of the TV camera, and the accumulation is over as soon as the wire leaves the area (Fig.1b). During the scanning time a charge is accumulated on the target, which is the image of the beam density distribution. The image on the vidicon of the TV camera operating in the storage (accumulation) mode is similar to the process on a photo film in the usual camera. Actually, the flying wire could be imagine as a fine "stationary screen" of wires (or foil). The information is read out from the TV camera and transferred to the computer right after the accumulation mode (Fig.1b).

The signal current of the vidicon is determined by the expression

$$i = M \frac{S_{TV}}{t_c} \frac{d}{V} \int \frac{d^2W}{d\lambda\, d\Omega} S_r(\lambda)\, d\lambda, \qquad (1)$$

where M is the optical transfer quotient, S_{TV} is the scanned area of the vidicon, t_c is the TV camera scan period, $d^2W/d\lambda d\Omega$ is the spectral-angular density of radiation, d is the wire cross section, V is the wire speed, $S_r(\lambda)$ is the radiant sensitivity, J is the particle current density in the accelerator. In our calculations we took the particle distibution in the accelerator follows to Gaussian.

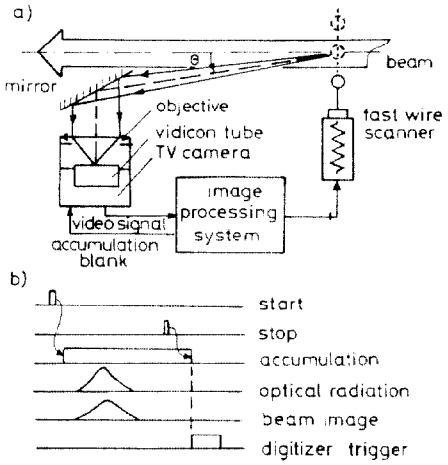

Fig. 1. The layout of the experimental facility (a) and the working algorithm of the measuring system (b).

Optical Radiation Sources

A luminescent wire with a high light yield and good radiation resistivety may be used as a scanning device. For instance the light yield of a wire 25 μm in diameter made from GSL (Ce) [5] is 1.5 photons/KeV, its decay time is 55 ns and the maximum of radiation occurs at the wave length 400 nm. The number of photons leaving the wire surface is 0.5 photons/sr·part. The heating of the wire caused by the beam may result in the attenuation of the luminescence. Therefore the range of its applicability is determined by the particle current low densities in the accelerator.

OTR is another important source of the optical radiation. OTR arises when a charged particle crosses the medium-vacuum boundary and decay time is very fast. In the case of relativistic particles the forward OTR is independent of the material properties, shape of the surface and temperature. This gives us a possibility to use the carbon or beryllium wires usually used in measurements.

The spectrum-angular distribution for the forward OTR for relativistic particles is described by the expression [6]

$$\frac{d^2N}{d\lambda\, d\Omega} = \frac{\alpha}{\lambda \pi^2} F(\theta), \quad F(\theta) = \frac{\theta^2}{(\gamma^{-2}+\theta^2)^2}, \qquad (2)$$

where $d^2N/d\lambda\, d\Omega$ is the number of photons with the wave length λ emitted into the solid angle unit Ω, θ is the angle between the radiation and the direction of particle motion. At the maximum OTR intensity the angle is equal $1/\gamma$. The results of the calculations made with formula (2) are presented in Fig.2.

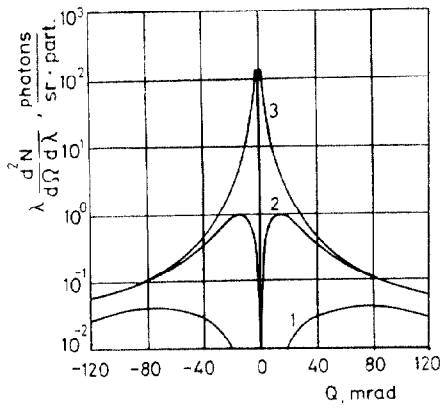

Fig. 2. Spectral-angular OTR distributions as different energies: 1 - 14 GeV, 2 - 70 GeV, 3 - 800 GeV.

As is seen from Fig.2 for the angles $\theta \gg 1/\gamma$ the value for OTR is practically independent of the particle energy. For example, for $\gamma \gg 70$ and the angle θ = =70 mrad the radiation intensity is equal to 0.13 protons/sr·part. within the wave range 300-700 nm. We have reliable experimental confirmations [6,7] of the fact that formula (2) describes nicely the OTR distribution at the particle interaction with thin films. At present there are neither experimental nor theoretical works, which describe OTR arising in the particle interaction with micro-objects. Rough estimates allow us to assume for the particle with γ =300 the transverse sizes of micro-objects should be larger than 20 μm. Therefore it is of practical importance to study experimentally OTR in the interaction of the particle with $\gamma > 300$ with objects of small sizes.

Since OTR is irradiated from the surface of the material, we have a possibility to use a ribbon of thin foil. This ribbon will make it possible to increase the integral luminosity and does not worsen the resolution. For instance, the foil 1 mm wide and 1 μm thick has the same cross section area as the wire of 35 μm diameter, but the light yield is 28 times higher than from the wire.

TV Camera

A digital television device with the vidicon LI-450 (XQ-1440) may be used as a detecting apparatus. It was used in the OTR investigations [6]. The cadmium selenid vidicon target possesses high quantum efficiency of 0.67, the sensitivity is $S_r(\lambda_m)$ =0.37 A/W in the maximum of the spectral charactersitics (λ_m = =680 nm).

The digital TV system with the vidicon LI-450 has the current noise 0.7 nA, which corresponds to 10^8 photons/cm^2. The TV cameras using SIT and ISIT - vidicons [8] are widely used for beam diagnostics purposes. These devices have a brightness intensification section and their threshold sensitivity is $4 \cdot 10^5$ and $2 \cdot 10^4$ photons/cm^2. Fig.3 shows the relative sensitivity for LI-450, SIT, SIT* (* - spectral characteristics correcred for the long wave range).

Heating

During beam scanning with the wire there occurs the radiation heating. The heated wire turns out to emit heat energy, which may cause to errors in measurements, sinece the shape of the temperature curve does not coincide with that of the beam. The temperature of the wire may be determined with the formula given in ref. 1 . However this formula does not take into account heat emission from the surface and the dependence of the thermal physical coefficients on temperature. Bearing in mind the importance of this problem, we have carried out numerical calculations.

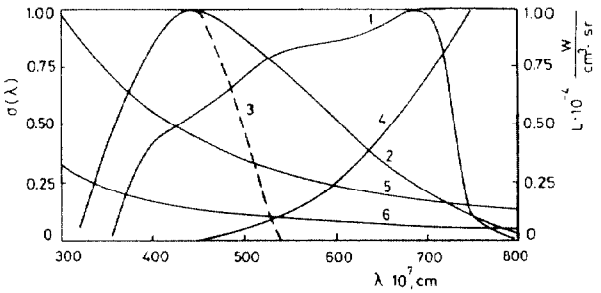

Fig. 3. Relative spectral characteristics: 1 - Li-450; 2 - SIT; 3 - SIT*; 4 - spectral brightness of a body at 1900° K, a=0.5; 5,6 - spectral OTR brightness at 67 mrad and γ =288 (5 - particle current density 0.44 A/cm^2, 6 - particle current density 0.14 A/cm^2).

During scanning the wire temperature first increase and then after reaching its maximum starts falling down. The value and position of the temperature maximum depend on many parameters, among them are the beam density, wire scanning speed and its sizes. Fig.4 presents a typical wire temperature dependence during scanning, as well as the values of the signals from the photoreceivers versus heat emission and OTR.

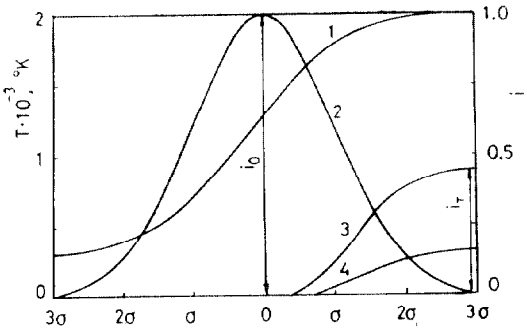

Fig. 4. Shapes of the photoreceiver signals, initiated by different types of radiation for CERN SPS (I=2·10^{13} p, E=270 GeV, σ =1.1 mm, d=25 μm, V=4.3 m/s): 1 - wire temperature when scanning; 2 - OTR signal at 67 mrad; 3 - relative value for LI-450 from heat emission; 4 - relative value for SIT signal from heat emission.

In order to describe the ratio between the useful and heat emissions we have introduced the parameter i_T/i_o, which is the ratio of the photoreceiver signal, initiated by the heat emission at the maximum temperature, to the useful emission signal in the beam centre. The beam will ultimately be distorted at the point where temperature reaches its maximum. The i_T/i_o parameter depends on the spectral characteristics of the photoreceiver, spectral composition of useful and heat emissions. Fig.3 presents the heat emission spectrum at 1900° K and OTR spectrum for two particle current densities in the machine. OTR at the angle of 67 mrad and beam current of 0.44 A/cm^2 initiates a similar signal in LI-450 as the wire heat emission at 1900°K. In the case of SIT the beam current value is 0.14 A/cm^2. The

SIT* characteristics corrected so as to improve the detection conditions. This reduces the device sensitivity by 30%, but the ratio i_T/i_o may be improved more than 10 times.

There are other ways to reduce the contribution from heat emission. For instance in the case of the bunched beams, one may use bunch selection, and for OTR it will be a polarized filter. It should be noted that this is the way to single out only heat emission of the wire and hence to obtain the information about the temperature regime of the wire when scanning.

It is a certain difficulty to give an analytic description of i_T/i_o because of a great number of the parameters in this formula. For the estimate of i_T/i_o one can use the plots presented in Fig. 5. Here the particle current in the machine has been found from the condition of equality of the transition radiation at the angle θ and heat emission with temperature T.

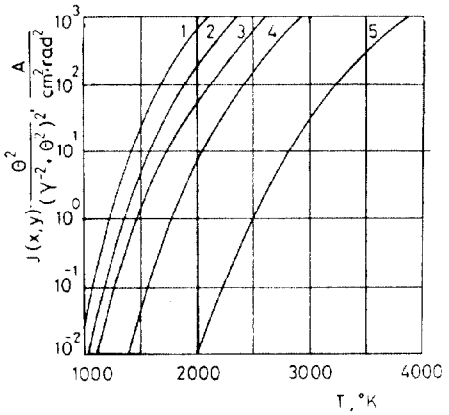

Fig. 5. The T-dependence of the particle current density, found from the condition of equality of the wire heat emission with a-0.5 and OTR for different types of detecting devices: 1 - λ = =700 nm, 2 - LI-450, 3 - SIT, 4 - SIT*, 5 - - λ =300 nm.

$$J=(x,y)F(\theta) = \frac{\int aL(\lambda, T)S_r(\lambda)d\lambda}{\int \xi(\lambda)\frac{\alpha}{\lambda\pi^2}S_r(\lambda)d\lambda}, \qquad (3)$$

where J(x,y) is the current density of a particle, $F(\theta)$ is a multiplier from formula (2), a is the dark quotient, $L(\lambda, T)$ is the brightness of heat emission of a black body, $\xi(\lambda)$ is the photon energy.

Results

The results for different machines IHEP, CERN, FNAL, KhPTI are given in Table. The following parameters have been calculated: I_{th} is the threshold sensitivity of the detectors (the number of particles in the accelerator causing the aappearance of a signal, equal to the device noise), T is the wire heating temperature, i_T/i_o is the relative values for the heat emission, as well as relative changes of the emittance $\Delta E/E$, momentum $\Delta P/P$ and beam losses $\Delta I/I$ as a result of scanning.

In the majority of cases the TV camera with LI-450 vidicon is capable of detecting the beam of high intensity. SIT guarantees the detection of separate bunches in the machine. ISIT allows one to control low intensity beams. For instance, in the case of the CERN antiproton beam a scanning device with detecting apparatus based on ISIT may be an alternative to the known techniques [10]. In this case the relative increase of the emittance will be not more than 1% the statistics measurement accuracy will be of about several percent.

Table

	U-70 [3]	UNK [3]	FNAL [3]	KhIPT [9]	CERN SPS [3]	CERN AA [10]	CERN AC [11]
Beam	p	p	p	e^-	p	p	p
γ	75	3200	853	3530	289	3.9	3.9
f, Hz	$2\cdot10^5$	$1.4\cdot10^4$	$4.7\cdot10^4$	100	$4.4\cdot10^4$	$1.8\cdot10^6$	$1.6\cdot10^6$
θ, mrad	70	70	70	70	67	268	268
σ_x, mm	3,0	1.0	0.3	1,0	1.1	1.4	3.8
σ_y, mm	1,7	5.0	0.3	1,0	1.1	1.4	3.8
I, part.	10^{13}	$2\cdot10^{14}$	$5\cdot10^{12}$	10 μA	$2\cdot10^{13}$	$6\cdot10^{11}$	$5\cdot10^7$
T, °K	1376	1433	1784	98	1709	1325	-
i_T/i_o							
LI-450	0,11	0.11	0.19	-	0.44	2.4	-
SIT	0,034	0.033	0.066	-	0.14	0.72	-
SIT*	$2\cdot10^{-3}$	$2\cdot10^{-3}$	$9\cdot10^{-3}$	-	0.018	0.035	-
I th, part.							
LI-450	$3.2\cdot10^9$	$4\cdot10^{10}$	$1.3\cdot10^9$	$4\cdot10^{-2}$ μA	$3\cdot10^9$	$5.6\cdot10^9$	-
SIT	$1.7\cdot10^7$	$2.2\cdot10^8$	$6.7\cdot10^6$	$2\cdot10^{-4}$ μA	$1.6\cdot10^7$	$3\cdot10^7$	$3.1\cdot10^5$
ISIT						$2.2\cdot10^6$	$1.6\cdot10^4$
E, π·mm·mrad						1	12
$\Delta E/E$						10^{-2}	10^{-2}
$\Delta N/N$						$7\cdot10^{-5}$	$4\cdot10^{-4}$
$\Delta P/P$						$4\cdot10^{-6}$	$3\cdot10^{-5}$

Notes: CERN AC - GS1(Ce^{3+}) wire, other machines - a carbon wire; KhTI - wire speed 10^{-2} m/s, for other machines - 4.3 m/s; CERN AC - wire diameter 10 μm, other machine - 25 μm.

References

1 J.Bosser et al. - CERN SPS/84-11.

2 R.E.Shaber//IEEE Trans. Nucl. Sci. NS-32, N5, p. 1862-1864.

3 V.T.Baranov et al. - Preprint IHEP 87-115, Serpukhov, 1987.

4 C.H.Steinbach, van M.Rolj. - CERN PS/95-33, 1985.

5 M.Atrinson et al.//NIM. 1987. V. A254, p. 500-514.

6 S.D.Borovkov et al. - Preprint IHEP 88-187, Serpukhov, 1988.

7 L.Wartski et al.//IEEE Trans. Nucl. Sci. 1975, NS-22, N3, p. 1552-1557.

8 R.Bossart et al.//NIM. 1981. V. 184, p. 349-357.

9 V.M.Denjak et al.//PTE. 1971. N4, p. 43.

10 H.Koziol. - CERN PS/AA/ME Note 26, April 30, 1982.

11 E.J.N.Wilson. - CERN 83-10. Proton Synchrotron Division, 26 October 1983.